

RESEARCH ARTICLE

Phospholipase C ϵ Modulates Rap1 Activity and the Endothelial Barrier

Peter V. DiStefano, Alan V. Smrcka, Angela J. Glading*

Department of Pharmacology and Physiology, University of Rochester, Rochester, New York, 14642, United States of America

* angela_glading@urmc.rochester.edu



OPEN ACCESS

Citation: DiStefano PV, Smrcka AV, Glading AJ (2016) Phospholipase C ϵ Modulates Rap1 Activity and the Endothelial Barrier. PLoS ONE 11(9): e0162338. doi:10.1371/journal.pone.0162338

Editor: Magdalena Chrzanowska-Wodnicka, BloodCenter of Wisconsin, UNITED STATES

Received: May 4, 2016

Accepted: August 22, 2016

Published: September 9, 2016

Copyright: © 2016 DiStefano et al. This is an open access article distributed under the terms of the [Creative Commons Attribution License](https://creativecommons.org/licenses/by/4.0/), which permits unrestricted use, distribution, and reproduction in any medium, provided the original author and source are credited.

Data Availability Statement: All relevant data are within the paper and its Supporting Information files.

Funding: This work was supported by National Institutes of Health grant HL117885-01 to A.J. Glading and American Heart Association predoctoral fellowship 14PRE2038009 to P.V. DiStefano. The funders had no role in study design, data collection and analysis, decision to publish, or preparation of the manuscript.

Competing Interests: The authors have declared that no competing interests exist.

Abstract

The phosphoinositide-specific phospholipase C, PLC ϵ , is a unique signaling protein with known roles in regulating cardiac myocyte growth, astrocyte inflammatory signaling, and tumor formation. PLC ϵ is also expressed in endothelial cells, however its role in endothelial regulation is not fully established. We show that endothelial cells of multiple origins, including human pulmonary artery (HPAEC), human umbilical vein (HUVEC), and immortalized brain microvascular (hCMEC/D3) endothelial cells, express PLC ϵ . Knockdown of PLC ϵ in arterial endothelial monolayers decreased the effectiveness of the endothelial barrier. Concomitantly, RhoA activity and stress fiber formation were increased. PLC ϵ -deficient arterial endothelial cells also exhibited decreased Rap1-GTP levels, which could be restored by activation of the Rap1 GEF, Epac, to rescue the increase in monolayer leak. Reintroduction of PLC ϵ rescued monolayer leak with both the CDC25 GEF domain and the lipase domain of PLC ϵ required to fully activate Rap1 and to rescue endothelial barrier function. Finally, we demonstrate that the barrier promoting effects PLC ϵ are dependent on Rap1 signaling through the Rap1 effector, KRIT1, which we have previously shown is vital for maintaining endothelial barrier stability. Thus we have described a novel role for PLC ϵ PIP₂ hydrolytic and Rap GEF activities in arterial endothelial cells, where PLC ϵ -dependent activation of Rap1/KRIT1 signaling promotes endothelial barrier stability.

Introduction

Phospholipase C (PLC) family members are common mediators of signal transduction in mammalian cells. Upon activation by growth factor receptors or G-protein coupled receptors, PLC cleaves phosphatidylinositol 4,5-bisphosphate (PIP₂), into inositol trisphosphate (IP₃) and diacylglycerol (DAG), which then mediate pleiotropic downstream effects on cell migration, proliferation, and cell contractility. There are six different sub-types of PLC, which all contain a conserved catalytic region, EF hand, and phospholipid binding domain[1,2]. PLC ϵ is unique among the PLC family as it possesses an N-terminal CDC25 GEF domain and two C-terminal Ras association (RA) domains, RA1 and RA2, allowing it to act as regulator and effector of Ras subfamily small GTPase signaling[1]. PLC ϵ has been shown to increase the exchange

of GDP for GTP in Rap1 via its CDC25 GEF domain [1,3]. Subsequently, Oestreich et al showed that basal Rap1 activity was diminished in PLC ϵ knockout hearts compared to wild type[4]. The RA2 domain, on the other hand, binds Rap1 and Ras and allows these proteins to stimulate the lipase activity of PLC ϵ [5–9]. The presence of these small GTPase signaling domains in PLC ϵ suggests that it acts as a specific link between GF/GPC receptor activity and Ras family GTPases. However, the role of PLC ϵ in regulating small GTPase signaling has only been explored in a few cellular contexts.

Rap1 GTPase is a master regulator of cell adhesion, including both cell-matrix and cell-cell adhesion. Its activity is tightly controlled by the combined action of Rap1 exchange factors (GEFs) and activating proteins (GAPs), which promote or reduce the amount of active, GTP bound, Rap1. In cultured endothelial cells, activation of Rap1 is essential for the formation of cell-cell junctions and baseline barrier function[10], and decreasing Rap1 activity via knockdown of PDZ-GEF or by expressing Rap1-GAP decreases endothelial barrier integrity[11,12]. Deletion of both Rap1 isoforms *in vivo* leads to hemorrhage, vascular rupture, and microvessel dilation, though with incomplete penetrance of the phenotype[13]. These data indicate that Rap1 activity is a major regulatory focus for endothelial barrier function, and suggest that the consistent maintenance of basal Rap1 activity may be a critical component of vascular homeostasis.

Rap1 is known to modulate endothelial cell-cell contacts via interactions with a number of proteins. Of these, it has recently emerged that Krev Interaction Trapped 1 (KRIT1) is essential for the ability of active Rap1 to stabilize endothelial cell-cell junctions, both at a basal level and downstream of a number of stimuli[12,14,15]. KRIT1 is a scaffold protein that co-localizes with β -catenin at areas of cell-cell contact[12]. Activation of Rap1 promotes KRIT1 membrane localization and junctional stability that is dependent on KRIT1-Rap1 binding[14]. KRIT1 expression is required for the ability of Rap1 to limit thrombin-induced leak [12], and reduced KRIT1 expression *in vitro* and *in vivo* destabilizes the endothelial barrier[12,16–18]. Another recent study has shown that the barrier-promoting properties of prostacyclin, which are known to occur via Rap1 activation, requires the Rap1-binding capacity of KRIT1[15]. This evidence suggests that the Rap1-KRIT1 signaling axis is a common component of endothelial barrier stabilization pathways. However, it is not known whether PLC ϵ , which can regulate Rap1 activity, can effectively regulate endothelial barrier stability, nor whether this requires the presence of KRIT1.

In this study we show that PLC ϵ is expressed abundantly in primary endothelial cells and endothelial cell lines, and that loss of PLC ϵ protein expression is sufficient to reduce the integrity of an endothelial monolayer. Reduced endothelial barrier function corresponded with increased Rho-GTP levels and cytoplasmic stress fiber formation, and with decreased Rap1 activity. Structure function experiments revealed that a CDC25-deficient PLC ϵ was unable to rescue the effect of PLC ϵ depletion on monolayer integrity. We were surprised to find that a mutant PLC ϵ lacking lipase activity also could not fully rescue endothelial monolayer integrity, and exhibited a moderate inhibitory effect on Rap1-GTP levels. Finally, we demonstrate that loss of the Rap1 effector, KRIT1, does not increase monolayer leak in PLC ϵ -deficient cells, suggesting that PLC ϵ and KRIT1 are acting in the same pathway. Together, our findings strongly suggest that PLC ϵ promotes endothelial barrier integrity by maintaining basal levels of Rap1-GTP through its lipase and CDC25 GEF domain, feasibly through promoting KRIT1 membrane localization and subsequent stabilization of endothelial cell-cell contact.

Experimental procedures

Ethics Statement

The isolation of neonatal rat ventricular fibroblasts was carried out in accordance with the recommendations of the NIH Guide for the Care and Use of Laboratory Animal and approved by

the University Committee on Animal Resources of the University of Rochester (Protocol number 2007-137R issued to Alan V. Smrcka).

Cell Culture and Transfection

HPAEC (Invitrogen, Carlsbad, CA), hCMEC/D3 (gift of Dr. Babette Wesker, Weil Cornell Medical College), and HUVEC (Lonza, Basel, Switzerland) were cultured in 1:1 Dulbecco's modified Eagle's medium (DMEM): F/12, supplemented with 5% fetal bovine serum (FBS), 1% endothelial cell growth supplement (ECGS, ScienCell, Carlsbad, CA), 1% antimyotic/antibiotic solution (Gibco/Invitrogen), and 50 μ M heparin (Calbiochem, La Jolla, CA), at 37°C with 5% CO₂. HPAEC were grown on 2 μ g/cm² gelatin coated tissue culture plates and only passages 3–6 were used in experiments. Neonatal rat ventricular fibroblasts were isolated from wildtype Sprague-Dawley rats and lysed in Laemelli buffer. HPAEC were transfected with 30ng siRNA using the HiPerfect transfection reagent (Qiagen, Valencia, CA) as reported previously [12,19]. Transfection efficiencies ranged from 80–95% based on transfection of fluorescently labeled siRNAs (data not shown).

Isolation of Neonatal Rat Ventricular Fibroblasts

Neonatal Rat Ventricular Fibroblasts were isolated from P2 Sprague-Dawley rat pups (Harlan Sprague-Dawley Inc./Envigo, Indianapolis, Indiana) that were sacrificed by immersion in 70% ethanol, followed by decapitation. Briefly, the hearts were excised and the ventricles were separated and minced in Hank's buffered salt solution (HBSS) containing CaCl₂ and MgCl₂ (Invitrogen) supplemented with 0.1% BSA (Sigma) and penicillin/streptomycin (Invitrogen), followed by three rounds of digestion with 250U/mg collagenase Type 2 (Worthington, Lakewood, NJ). The digestion mixture was spun down and the cell containing pellet was resuspended in DMEM (Lonza) supplemented with 2mM L-glutamine (Invitrogen), 2% penicillin/streptomycin, 200 ng/ml Vitamin B12 (Sigma), and 10% FBS, and pre-plated on an uncoated tissue culture dish for 1 hour. Myocytes were washed off the plate and the adhered fibroblasts were expanded for 3 days, then lysed in Laemelli buffer for Western blot.

siRNA and Plasmids

Non-targeting negative control siRNA #1 and anti-KRIT1 siRNA (AM16708, Ambion/Invitrogen) were used as reported previously [12,19]. Knockdown efficiency was measured in each experiment by protein detection of KRIT1, as indicated in the appropriate figures.

Adenovirus Infection

To generate the PLC ϵ Δ CDC25/lipase dead clone (Δ CDC25/LD), the N-terminal cDNA of PLC ϵ lipase dead was digested with NheI and NdeI and replaced with the corresponding region of PLC ϵ Δ CDC25 in pShuttle-CMV. The identity of the clone was confirmed by restriction digestion, sequencing, and Western blotting. Adenovirus for this construct was generated in the same manner used to generate the PLC ϵ Δ CDC25, PLC ϵ lipase dead (LD), PLC ϵ K2150E, PLC ϵ siRNA, random siRNA, and PLC ϵ siRNA resistant (WT) adenoviruses as reported previously [4,5,20,21]. HPAEC were infected with 60 m.o.i of random, PLC ϵ siRNA, or siRNA resistant PLC ϵ or 120 m.o.i of PLC ϵ Δ CDC25, PLC ϵ lipase dead, PLC ϵ K2150E, or PLC ϵ Δ CDC25/lipase dead for 4 hours followed by a medium change.

Immunoprecipitation and Western Blotting

Cells were treated with or without 1 μ M 8-pCPT-2'-O-Me-cAMP-AM (Tocris/R&D Biosystems) as indicated in the figure legends. Lysates were prepared as reported previously [12].

KRIT1 was immunoprecipitated using 2 μ g monoclonal anti-KRIT1 (EMD Millipore, Darmstadt, Germany). Lysates were probed with polyclonal rabbit anti-KRIT1 Δ 6832 (Ginsberg Lab, UCSD) at a dilution of 1:1000. Control lysates were immunoprecipitated with mouse non-immune IgG (Santa Cruz, Dallas, TX). Antibodies used for Western blot were rabbit anti-actin (Sigma, St. Louis, MO), rabbit anti-GAPDH (Santa Cruz), rabbit anti-PLC ϵ (Smrcka Lab, University of Rochester), and rabbit anti-VE cadherin (Cayman Chemical, Ann Arbor, MI). The secondary antibodies used were goat anti-rabbit Dylight-680 (Thermo Fisher Scientific) and goat-anti rabbit 800 (Fisher). An Odyssey Infrared Imaging System (LI-COR Biosciences, Lincoln, NE) was used to image membranes and for densitometry.

Endothelial Monolayer Leak Assay

HPAECs were plated onto 3 μ m pore polyester transwell filters (Corning Life Sciences, Corning, NY) coated with 10 μ g/ml human plasma fibronectin (gift from Dr. Denise Hocking, University of Rochester). Cells were infected with adenovirus 24 hours after plating and grown for 72 hours at 37°C to full confluence. Cells were then incubated in DMEM with 0.5% FBS for 2 hours, then treated with or without 8-pCPT-2'-O-Me-cAMP-AM (1 μ M) for 30 minutes. Horseradish peroxidase (HRP, 1.5 μ g/ml, Sigma) was added to upper wells, and the plates were then incubated for an additional 2 hours at 37°C. The HRP content of the lower chamber medium was then measured using a 3,3', 5,5'-tetramethylbenzidine (TMB, eBioscience, San Diego, CA) colorimetric assay. Briefly, 10 μ l samples of the lower chamber medium were transferred in triplicate to a 96well plate. 100 μ l of TMB was added to each sample and the reaction was allowed to proceed for 1 min. A standard curve of HRP from 0 to 0.5 μ g/ml was run alongside experimental samples. The reaction was stopped by adding 100 μ l 1N HCL to each well. Absorbance at 450nm was acquired and raw absorbance values were converted into concentrations using the standard curve. After samples were removed, the transwell filters were fixed in 4% formaldehyde (Fisher), stained with 0.25% Coomassie blue (Bio-Rad, Hercules, CA), and examined to confirm the integrity of each cell monolayer. Alternatively, 1 mg/ml fluorescein isothiocyanate-dextran of 4, 70, or 150 kDa molecular weight (FITC-dextran, Sigma) was added to the top chamber \pm 4U/ml thrombin (Sigma). At the reported time intervals, 50 μ l samples were taken from the bottom chamber and fluorescence was measured at excitation 485 nm/emission 520 nm on a Synergy H4 hybrid plate reader (Biotek, Winooski, VT). Data were analyzed using one-way ANOVA with Tukey's post-hoc testing.

Immunofluorescence

Cells were infected 24 hours after plating on 10 μ g/ml fibronectin coated glass coverslips and allowed to grow for an additional 48 hours to confluence, then treated with or without 1 μ M 8-pCPT-2'-O-Me-cAMP-AM. Cells were fixed with 4% formaldehyde for 20 minutes, permeabilized for 5 minutes with 0.2% Triton-X-100, then blocked with 10% normal goat serum for 1 hour. Cells were then incubated with 1:300 rabbit anti-VE-cadherin (Cayman Chemical), followed by incubation with 1:500 goat anti-rabbit IgG 488 (Invitrogen). Cells were counterstained with 1 μ g/ml Hoechst (Invitrogen) for 5min prior to mounting. VE-cadherin staining was quantified by measuring the width of half-maximal VE-cadherin staining intensity at cell borders using ImageJ.

F-actin quantitation

Cells were incubated with 14 μ M rhodamine-phalloidin (Cytoskeleton, Denver, CO) for 30 minutes on ice then counterstained with 1 μ g/ml Hoechst. Images were captured at room temperature using Metamorph software (Molecular Devices, Sunnyvale, CA) with an UPLSAPO 20x

(n.a. 0.75) objective on an Olympus IX81 microscope, and an ORCA-ER digital camera (Hamamatsu, Hamamatsu City, Japan). Images were imported into ImageJ for further analysis. Cytoplasmic F-actin fluorescence intensity was calculated along a line scan drawn perpendicular to the main cell axis as reported in (16). Cortical actin intensity along the cell edge was calculated in a similar manner, with the line drawn perpendicular to the cell edge and to the main cell axis, incorporating the junction between two cells but no more than 15% of the width of the cytoplasm. Intensity values were obtained by integrating the area under the curve of the intensity histogram generated by the line scan. The area calculated was then divided by length of the line scan, yielding an average intensity value. Data were analyzed using one-way ANOVA with Tukey's post-hoc testing.

Small GTPase Pulldowns

After stimulation with or without 1 μ M 8-pCPT-2'-O-Me-cAMP-AM, cells were lysed in MgALB lysis buffer (50mM Tris HCl pH 7.5, 200mM NaCl, 2mM MgCl₂, 10% glycerol, 1% NP-40) or 1X RIPA lysis buffer, for Rap1 and RhoA pulldowns respectively. Lysates were clarified at 14,000 RPM for 5 minutes followed by incubation with 20 μ g GST RalGDS-RBD or GST rhotekin-RBD immobilized on GSH-sepharose for 45 minutes at 4°C. Afterwards, the sepharose beads were washed 3X with lysis buffer, re-suspended and boiled in 2X reducing Laemmli buffer, and centrifuged. Supernatant was then loaded on SDS PAGE gel for Western blot analysis. Mouse anti-Rap1 (Santa Cruz) and mouse anti-RhoA (Cytoskeleton) were used at 1:500 followed by incubation with a 1:5000 dilution of HRP conjugated goat anti-mouse IgG. Blots were developed using CL-XPosure film (Thermo Fisher Scientific) and analyzed using Image Studio Lite software (LI-COR Biosciences).

Statistics

Statistical analysis (i.e. one-way ANOVA with appropriate post-hoc testing) was performed using PRISM software (version 4.0, GraphPad Software Inc., La Jolla, CA). Significance was set at $\alpha = 0.05$.

Results

PLC ϵ is highly expressed in the endothelium and limits monolayer leak

PLC ϵ has been reported to be expressed endogenously in a multitude of cell types including Rat-1 fibroblasts, astrocytes, pancreatic beta cells, mouse ventricular myocytes, and neonatal rat ventricular myocytes [22–25]. Expression of PLC ϵ mRNA has been reported in freshly isolated murine endothelial cells but not HUVEC [26,27]. We detected high levels of PLC ϵ protein in endothelial cells from multiple origins, including HPAEC, HUVEC, and immortalized brain microvascular endothelial cells (hCMEC/D3, Fig 1A). The anti-PLC ϵ antibody, which recognizes the RA2 domain of PLC ϵ [25], detected a doublet at approximately 254 and 221 kDa (Fig 1A), corresponding to the splice variants of PLC ϵ , PLC ϵ 1a and PLC ϵ 1b, which differ in the number of amino acids N-terminal to the CDC25 domain [25,28]. The molecular weight of the bands matched those seen in neonatal rat ventricular fibroblasts (NRVF) and the upper band was significantly enhanced in HPAEC over-expressing PLC ϵ 1a. No bands were detected in PLC ϵ knockout heart lysate (Fig 1A).

To examine the role of PLC ϵ in endothelial cells, we knocked down PLC ϵ expression using virally delivered anti-PLC ϵ siRNA, which targets the RA1 domain [21,24]. Western blotting confirmed that 60 m.o.i. reduced PLC ϵ 1a protein expression by 70% and PLC ϵ 1b expression by 50% (Fig 1B). We could restore PLC ϵ expression by co-infection with siRNA resistant wild

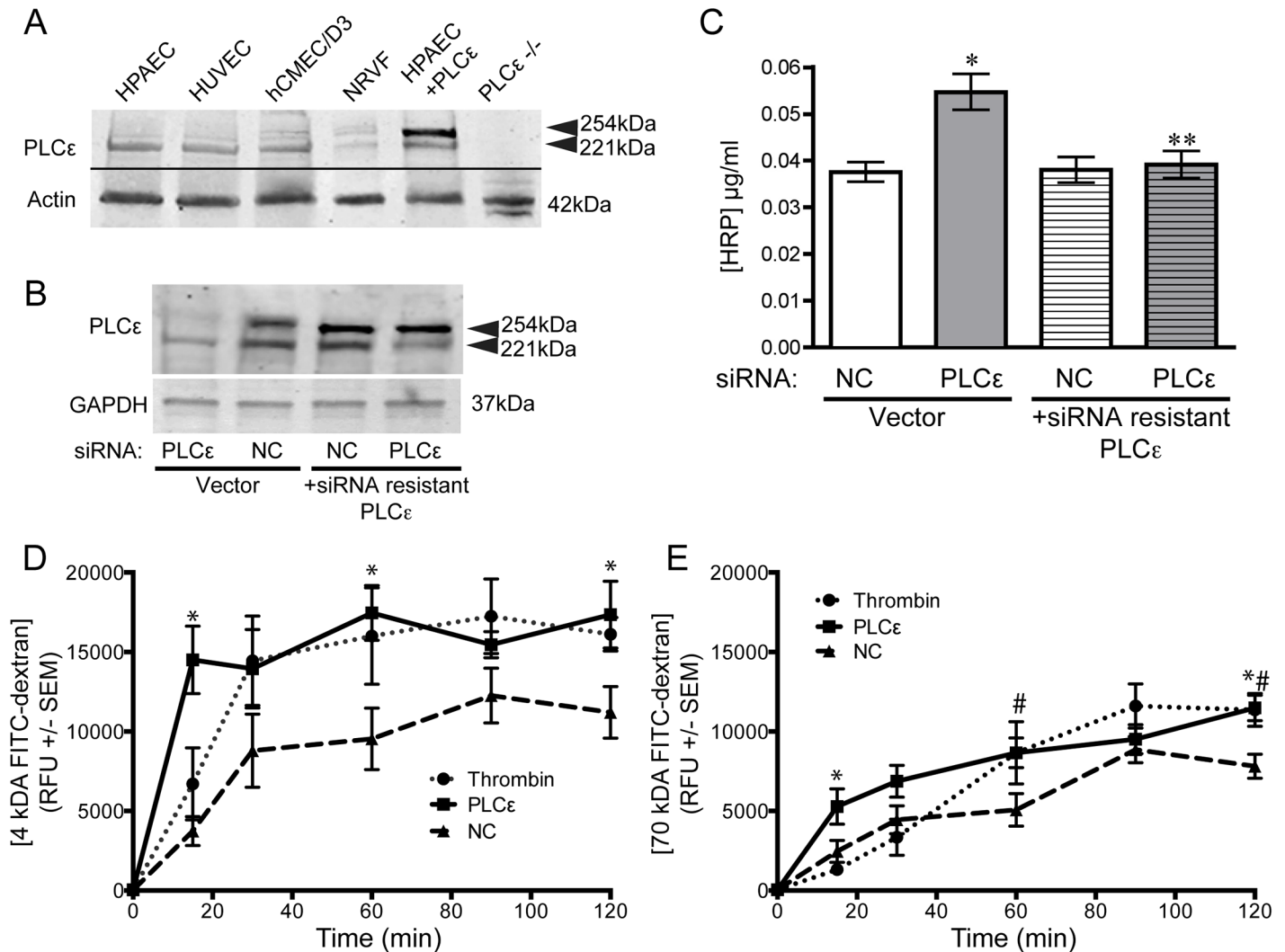


Fig 1. PLCε is expressed in endothelial cells and limits monolayer leak. **A)** PLCε expression in equivalent amounts of endothelial, NRVF, and heart lysate. HPAEC+ PLCε, HPAEC over-expressing PLCε; PLCε^{-/-}, PLCε knockout heart lysate. Blots are representative, n = 3. **B)** PLCε expression in HPAEC infected with random siRNA (negative control, NC) or PLCε siRNA ± siRNA resistant PLCε. Blots are representative, n = 3. **C)** HRP leak through a HPAEC monolayer infected with negative control (NC) or PLCε siRNA ± siRNA resistant PLCε. Data shown are mean HRP concentration, ± SEM. n = 6, p < 0.0001 by ANOVA, *p < 0.001 by post-hoc test vs. NC infected cells and **p < 0.001 vs. PLCε siRNA infected cells. **D)** Leak of 4 kDa FITC-dextran through an HPAEC monolayer infected with negative control (NC) ± 4U/ml thrombin or PLCε siRNA. Data shown are relative fluorescence units (RFU), ± SEM, n = 8. *p < 0.05 PLCε siRNA vs. NC by 2-way ANOVA. **E)** Leak of 70 kDa FITC-dextran through an HPAEC monolayer infected with negative control (NC) ± 4U/ml thrombin or PLCε siRNA. Data shown are RFU ± SEM, n = 8. *p < 0.05 PLCε siRNA vs. NC, #p < 0.05 thrombin vs. NC, by 2-way ANOVA.

doi:10.1371/journal.pone.0162338.g001

type PLCε1a (Fig 1B). We then examined a key endothelial phenotype, barrier stability, in PLCε depleted cells, using a transwell leak assay. Knockdown of PLCε increased the leak of horseradish peroxidase (HRP, ~30kDa) 1.7-fold over random-siRNA infected cells. siRNA specificity was confirmed by rescuing monolayer barrier function via re-expression of siRNA resistant wild type PLCε (Fig 1C). PLCε knockdown also increased the diffusion of both 4- and 70kDa FITC-labeled dextran through the monolayer compared to control siRNA infected cells. As shown in Fig 1D, 4kDa FITC-dextran moves across the monolayer rapidly in both PLCε siRNA and thrombin treated cells, reaching equilibrium within 30 minutes. Comparatively, flux of 70kDa FITC-dextran occurs at a much slower rate, with equilibrium not reached after 2hr. Notably, the rate of flux for both dextran sizes was similar in PLCε siRNA treated cells

and cells treated with thrombin. Indeed, both thrombin and PLC ϵ siRNA were not able to significantly increase the flux of 150kDa FITC-dextran (S1 Fig), suggesting the 'pore size' generated by knockdown of PLC ϵ has a finite range.

Depletion of PLC ϵ activates RhoA and leads to cytoskeletal rearrangement in HPAEC

Endothelial monolayer leak is commonly associated with an increase in the activity of the small GTPase, RhoA. RhoA-GTP activates Rho-associated protein kinase, which subsequently phosphorylates myosin light chain to increase actin-myosin contraction and increase the formation of transverse cellular actin bundles (stress fibers, [29]). The subsequent increase in cellular tension exerts a negative influence on the stability of cell-cell contacts. RhoA-mediated increased cellular contractility occurs under many conditions that increase endothelial leak. Therefore, we examined RhoA activity and the morphology of the actin cytoskeleton in PLC ϵ -deficient cells. RhoA activity increased approximately two-fold in PLC ϵ -deficient cells over control cells (Fig 2A and 2B). While large transverse stress fibers are a hallmark of RhoA activation[30], when we examined the morphology of the actin cytoskeleton, a large proportion of PLC ϵ depleted cells exhibited extremely short, stubby perinuclear stress fibers that are relatively atypical of activation of RhoA (Fig 2C). Quantitation of the distribution of actin fibers in the cells, however, clearly shows an increase in cytoplasmic actin staining in the endothelial monolayer, indicative of an increase in cellular contractility, as well as a decrease in cortical actin intensity (Fig 2D–2G).

Next, we asked whether increasing Rap1 activity through the Rap1 GEF, Epac, which acts independently of PLC ϵ , could reverse the increase in RhoA activity. We and others have demonstrated that RhoA activation can be inhibited by active Rap1 [10,12], suggesting that the activation of RhoA in PLC ϵ -deficient cells could be due to a loss of Rap1 activity. Treatment of PLC ϵ depleted cells with 8-pCPT-2'-O-Me-cAMP-AM, a potent and specific Epac activator[31], successfully reduced the amount of active RhoA down to control levels (Fig 2A), and reversed the stress fiber phenotype (Fig 2E–2G), indicating that loss of Rap1 activation could account for the increase in RhoA activity.

Reduced active Rap1 levels following depletion of PLC ϵ is responsible for monolayer leakiness

The finding that activation of Rap1 was able to reverse the increased RhoA activity in PLC ϵ -deficient cells suggested that basal Rap1 activity is reduced in PLC ϵ -deficient cells, similar to what has been reported in PLC ϵ knockout mouse hearts[4]. Knockdown of PLC ϵ in HPAEC decreased active Rap1 levels 50% compared to control cells, which could be restored by 8-pCPT-2'-O-Me-cAMP-AM stimulation (Fig 3A and 3B). Correspondingly, treatment of PLC ϵ -deficient endothelial cells with 8-pCPT-2'-O-Me-cAMP-AM was also able to prevent increased monolayer leak (Fig 3C), indicating that the loss of Rap1 activity was responsible for the appearance of these phenotypes. As Rap1 activation stabilizes junctional VE-cadherin through its effector KRIT1 [19], we also examined VE-cadherin expression and localization. Knockdown of PLC ϵ did not significantly alter VE-cadherin expression (S2 Fig) but reduced the intensity of VE-cadherin staining at cell junctions compared to control siRNA infected cells (Fig 3D and S2 Fig). This decrease was reversed following treatment with 8-pCPT-2'-O-Me-cAMP-AM, suggesting that loss of Rap1 activity in PLC ϵ deficient cells leads to the reduction in VE-cadherin at sites of cell-cell contact.

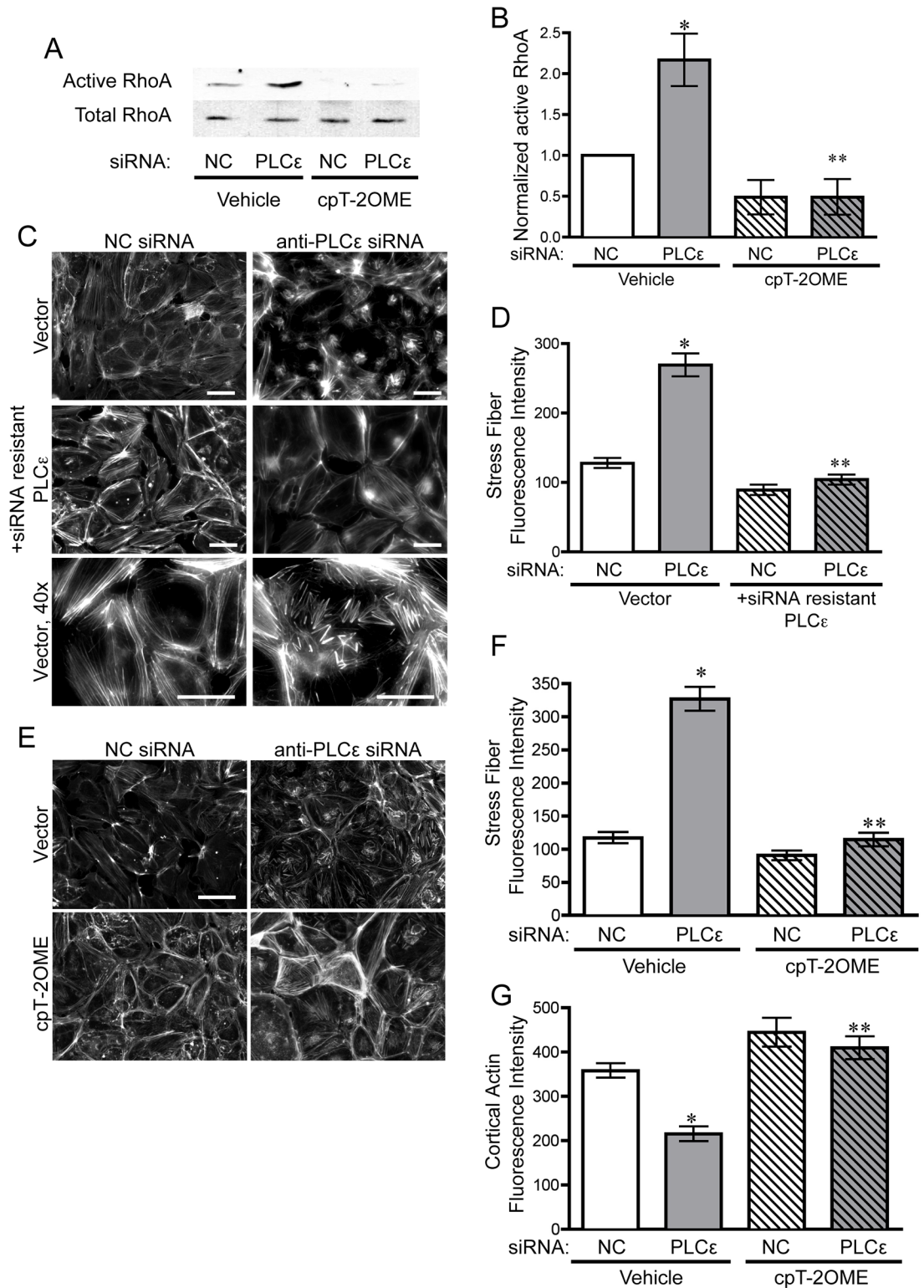


Fig 2. PLCε depletion leads to increased RhoA activity and stress fiber formation. **A**) Active RhoA pulldown assay from lysates infected with negative control (NC) or PLCε siRNA ± 1 μM 8-pCPT-2'-O-Me-cAMP-AM (cpT-2OME). Blots are representative, n = 4. **B**) Densitometric quantification of blots in (A). Data shown are active RhoA normalized to total RhoA ± SEM, n = 4, p = 0.0005 by ANOVA, *p < 0.05 vs. NC infected cells, and **p < 0.001 vs. PLCε siRNA infected cells by Tukey's Multiple Comparison Test. All blots used for this quantification can be found in [S5 Fig](#). **C**)

Rhodamine-phalloidin stained HPAEC infected with NC or PLCε siRNA ± siRNA resistant PLCε. Scale bar = 50μm. Images are representative of 3 separate experiments. **D**) Fluorescent intensity quantification of (C). $n \geq 40$ cells from 10 fields of view, $p < 0.0001$ by ANOVA, $*p < 0.001$ by post-hoc test vs. NC infected cells. $**p < 0.001$ vs. PLCε siRNA infected cells. **E**) Epifluorescence images of rhodamine-phalloidin stained HPAEC infected with negative control (NC) or PLCε siRNA ± 1μM 8-pCPT-2'-O-Me-cAMP-AM. **F**) Fluorescent intensity quantification of cytoplasmic stress fibers (E). $n \geq 40$ cells from 10 fields of view, $p < 0.0001$ by ANOVA, $*p < 0.001$ by post-hoc test vs. NC infected cells. $**p < 0.001$ vs. PLCε siRNA infected cells. **G**) Fluorescent intensity quantification of cortical actin in (E). $n \geq 40$ cells from 10 fields of view, $p < 0.0001$ by ANOVA, $*p < 0.001$ by post-hoc test vs. NC infected cells. $**p < 0.001$ vs. PLCε siRNA infected cells.

doi:10.1371/journal.pone.0162338.g002

The CDC25 and lipase activity of PLCε maintain active Rap1 levels and limit monolayer leak and stress fiber formation

The CDC25 domain of PLCε has been reported to function as a Rap1 GEF, leading to increased Rap1 activity when overexpressed with Rap1 in COS-7 cells, as well as increased GDP release

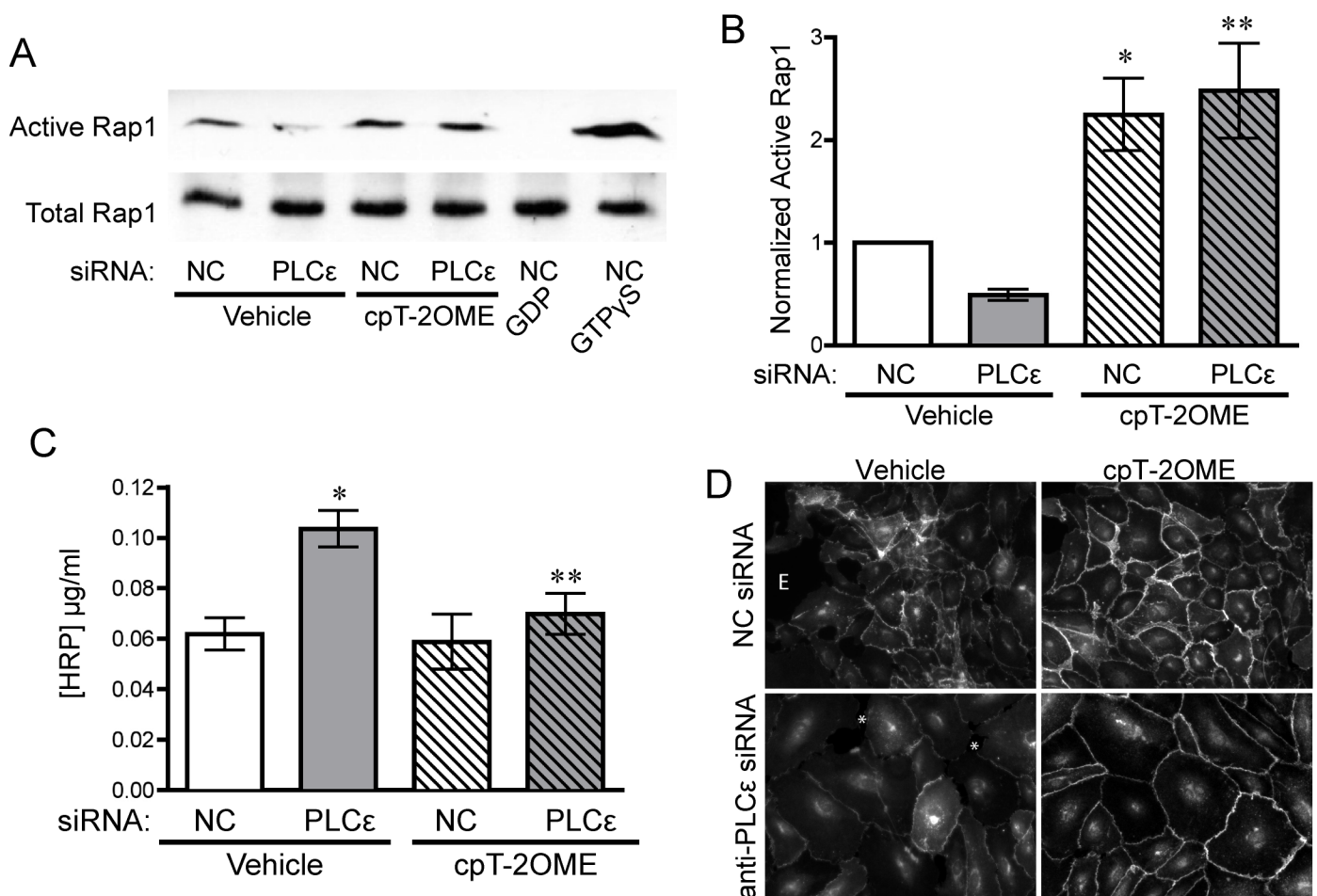


Fig 3. PLCε depletion leads to decreased basal Rap1 activity, which drives monolayer leak. **A**) Active Rap1 pull-down assay from lysates infected with negative control (NC) or PLCε siRNA ± 1μM 8-pCPT-2'-O-Me-cAMP-AM (cpT-2Ome), 1mM GDP, or 100μM GTPγS. Blots are representative, $n = 7$. **B**) Densitometric quantification of blots in (A). Data shown are active Rap1 normalized to total Rap1 ± SEM, $n = 7$, $p = 0.0001$ by ANOVA, $*p < 0.05$ vs. NC infected cells by post-hoc test, and $**p < 0.05$ vs. PLCε siRNA infected cells. All blots used for quantification can be found in [S6 Fig](#). **C**) HRP leak through HPAEC monolayer infected with NC or PLCε siRNA ± 1μM 8-pCPT-2'-O-Me-cAMP-AM. Data shown are the mean HRP concentration, ± SEM. $N = 5$, $p = 0.0022$ by ANOVA, $*p < 0.001$ by post-hoc test vs. NC infected cells and $**p < 0.05$ vs. PLCε siRNA infected cells. **D**) VE-cadherin stained HPAEC infected with negative control or PLCε siRNA ± 1μM 8-pCPT-2'-O-Me-cAMP-AM (cpT-2Ome). * indicates gaps occurring between endothelial cells. E- edge of monolayer. Images are representative of 3 separate experiments.

doi:10.1371/journal.pone.0162338.g003

in an in vitro GEF assay[3]. To confirm that the CDC25 domain of PLC ϵ was responsible for maintaining basal Rap1-GTP levels in our system, and determine whether this domain is necessary for stabilizing endothelial barrier function, we expressed a PLC ϵ mutant lacking the CDC25 GEF domain (Δ CDC25) in PLC ϵ -deficient HPAEC (Fig 4A). Reconstitution of PLC ϵ -deficient HPAEC with the Δ CDC25 mutant was not able to rescue decreased Rap1-GTP levels (Fig 4B and 4C) and was unable to reverse the increase in monolayer leak or the changes in actin cytoskeletal morphology (Fig 4D–4F). While it appeared that Δ CDC25 increased barrier function slightly, there was no statistical difference between PLC ϵ siRNA transfected cells with or without co-expression of Δ CDC25 (Fig 4D). In addition, Δ CDC25 appeared to have a slight dominant negative effect in control cells, but that also did not reach statistical significance. Rap1 can also interact with the C-terminal RA2 domain of PLC ϵ [8]. However, a PLC ϵ construct with a binding-defective RA2 domain[5] was able to efficiently rescue monolayer leak and had no effect on Rap1-GTP levels (S3 Fig).

As an additional control, we re-expressed a PLC ϵ mutant lacking lipase activity (LD, Fig 5A). Unexpectedly, the lipase dead mutant also could not fully rescue monolayer leak (Fig 5B), despite equivalent protein expression, suggesting that both the GEF domain and lipase activity of PLC ϵ are important for maintaining endothelial junctional stability. PLC ϵ -LD transfected cells also exhibited a decrease in Rap-GTP and abnormal stress fiber morphology (Fig 4B, 4C, 4E and 4F), which corresponded with the impairment of barrier function. Because both the Δ CDC25 mutant and the lipase dead mutant appeared to partially rescue barrier function, we elected to make a PLC ϵ mutant lacking both the CDC25 domain and lipase activity (Δ CDC25/LD, Fig 5C). This double mutant completely lacked any ability to rescue Rap1 GTP levels (Fig 5D and 5E), monolayer leak (Fig 5F), or stress fiber formation (Figs 4F and 5G) in PLC ϵ -deficient HPAEC, lending extra support to the idea that both of these domains are involved in the regulation of Rap1 activity and maintenance of endothelial cell-cell contacts.

PLC ϵ lies upstream of KRIT1 signaling, through which it maintains barrier integrity

The Rap1 effector, KRIT1, is vital for maintaining endothelial barrier stability, and acts as an endogenous inhibitor of junctional RhoA signaling[12,17,32]. Rap1-GTP promotes KRIT1 association with adherens junction complexes where it is thought to elicit its barrier protective effects(13). We hypothesized that PLC ϵ -mediated activation of Rap1 would act through KRIT1 to stabilize the endothelial barrier. Knockdown of KRIT1 in PLC ϵ -deficient endothelial cells (S4 Fig) did not have an additive effect on monolayer leak, but prevented rescue by Epac activation (Fig 6A). In addition, siRNA resistant WT PLC ϵ could not rescue barrier function in PLC ϵ -deficient cells in the absence of KRIT1 (Fig 6B). Together, these data provide evidence that PLC ϵ lies upstream of KRIT1. In summary, our findings show that PLC ϵ can promote endothelial barrier integrity by maintaining basal levels of Rap1-GTP/KRIT1 through its lipase and CDC25 GEF domain.

Discussion

In this study, we have shown that PLC ϵ is abundantly expressed in endothelial cells and its depletion leads to decreased barrier integrity (Fig 1) in arterial endothelial cells. The decrease in barrier integrity corresponds with increased Rho activity and subsequent stress fiber formation (Fig 2). Our evidence suggests that the loss of barrier function and Rho activation is due to reduced basal levels of Rap1, and subsequent KRIT1 signaling downstream, following PLC ϵ knockdown (Figs 3 and 6). Surprisingly, both the CDC25 GEF domain and lipase activity of PLC ϵ appear important for maintaining barrier function and active Rap1 levels (Figs 4 and 5).

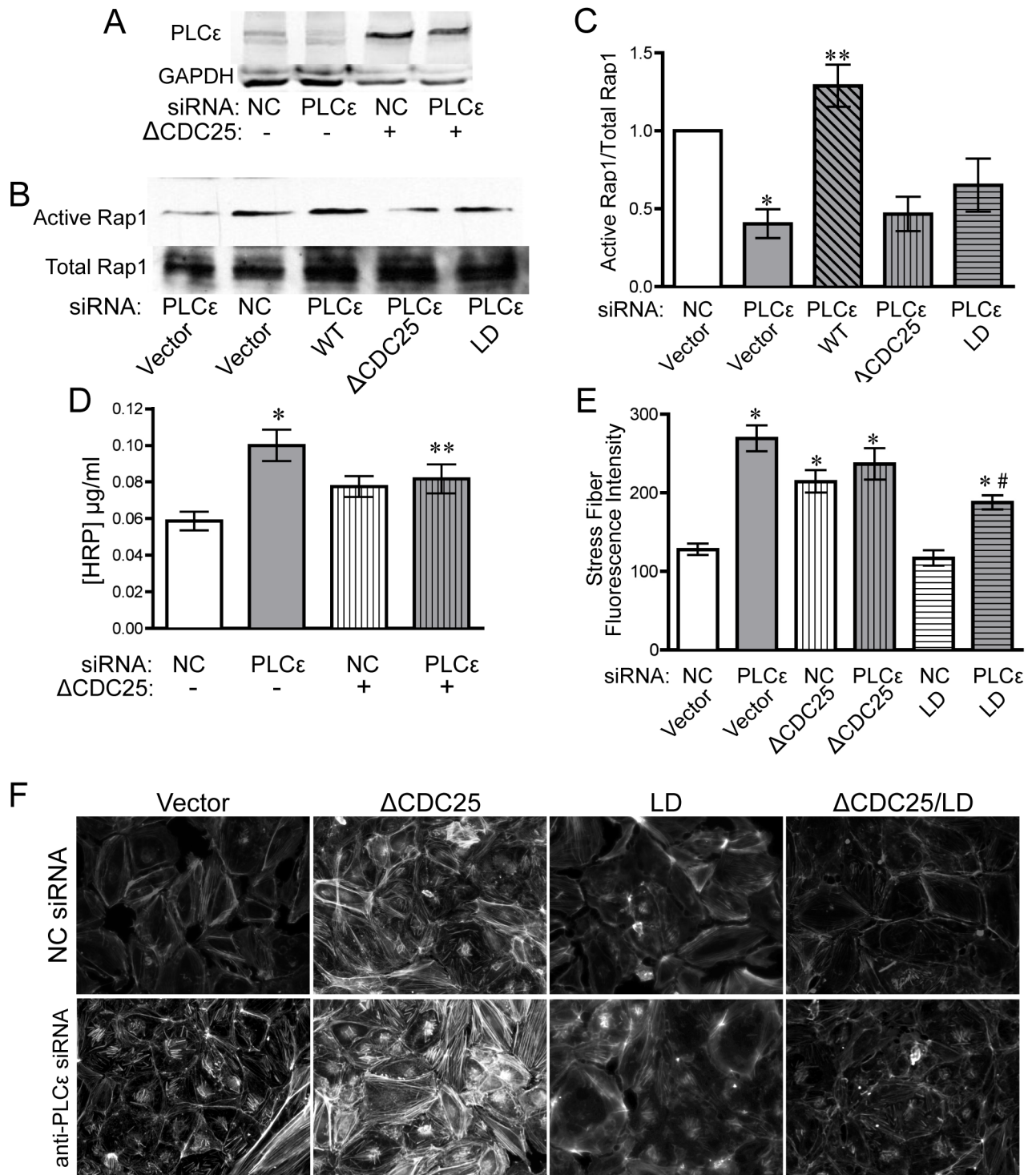


Fig 4. The CDC25 domain of PLCε maintains monolayer integrity and basal Rap1 activity. **A)** PLCε expression in HPAEC infected with NC or PLCε siRNA ± PLCε ΔCDC25. Blots are representative, n = 4. **B)** Active Rap1 pull-down assay from lysates infected with negative control or PLCε siRNA ± siRNA resistant PLCε (WT), PLCε ΔCDC25, or PLCε lipase dead (LD). Blots are representative, n = 5. **C)** Densitometric quantification of blots in (B). Data shown are active Rap1 normalized to total Rap1 ± SEM, n = 5, p = 0.0001 by ANOVA, *p < 0.01 vs. NC infected cells by post-hoc test, and **p < 0.001 vs. PLCε siRNA infected cells. All blots used for quantification can be found in [S7 Fig](#). **D)** HRP leak through HPAEC monolayer infected with negative control (NC) or PLCε siRNA ± PLCε ΔCDC25 (ΔCDC25). Data shown are the mean HRP concentration, ± SEM. n = 17, p < 0.0001 by ANOVA, *p < 0.001 by post-hoc test vs. NC infected cells and **p < 0.05 vs. NC infected cells. **E)** Fluorescent intensity quantification of actin staining in (F). n ≥ 40 cells from 10 fields of view, p < 0.0001 by

ANOVA, * $p < 0.001$ by post-hoc test vs. NC infected cells. # $p < 0.001$ vs. PLC ϵ siRNA infected cells. F) Epifluorescence images of rhodamine-phalloidin stained HPAEC infected with negative control or PLC ϵ siRNA \pm Δ CDC25, LD, or Δ CDC25/LD. Images are representative of 3 separate experiments.

doi:10.1371/journal.pone.0162338.g004

Together, our data suggest that PLC ϵ activity functions to sustain basal levels of Rap1 activity required for maintenance of basal endothelial barrier function. This is the first evidence, to our knowledge, that a PLC isoform can have a barrier protective effect in the endothelium. This runs contrary to the known effects of other members of this family, such as PLC β 3, which have been reported to increase endothelial permeability[33]. We believe this unique capability is due to the presence of the CDC25 Rap GEF domain. This suggests that activation of PLC ϵ may play a negative feedback role, limiting the loss of permeability in endothelial cells exposed to general PLC-activating signals.

While we fully expected that the CDC25 domain would be required, we were surprised to find that the lipase domain of PLC ϵ was also required to fully restore barrier function in PLC ϵ depleted cells. Lipase activity of other phospholipases has conventionally been associated with loss of endothelial barrier function[34–36]. Canonically, PLC lipase activity produces IP₃, which leads to increased intracellular calcium and DAG which, together with calcium, activates protein kinase C (PKC). Both calcium and PKC have been identified as second messengers in pathways which increase endothelial permeability[37–41]. However, some have suggested that in vivo, PKC activity is required to maintain basal levels of permeability, and conversely is not involved in inflammation-induced permeability[38]. Recent work from our laboratory supports the idea that PLC ϵ may signal primarily through PKC; PLC ϵ activity results in sustained production of DAG from PI₄P, rather than PIP₂, and thus sustained PKC activation[21,42]. During revision of this paper, Bijli, et al published that loss of PLC ϵ protects against vascular disruption and acute lung injury in response to lipopolysaccharide[43], suggesting that the role of PLC ϵ in regulating inflammation-induced endothelial permeability may be distinct from its role in modulating baseline endothelial permeability. As activation of Rap1 by Epac can prevent the loss of endothelial barrier function due to thrombin-dependent activation of RhoA (11), it may be the case that PLC ϵ acts through a Rap1-independent mechanism to regulate the endothelial response to inflammatory stimuli. Future experiments are necessary to explore the potential differences in signaling downstream of PLC ϵ under inflammatory vs. unstimulated conditions, particularly regarding the importance of sustained PKC activation.

Alternatively, the requirement for the lipase domain could be explained by cross-talk between the lipase domain and the CDC25 domain. Recently, Dusaban et al proposed a positive feedback mechanism whereby Rap1 activation by the CDC25 domain promotes Rap1 association with RA2, and a subsequent increase in PLC ϵ lipase activity[44]. While this feed-forward loop does not appear critical to endothelial barrier function, as a PLC ϵ construct containing a function blocking mutation of the RA2 domain was able to rescue all endothelial phenotypes associated with PLC ϵ depletion (S3 Fig), this mechanism does support the existence of autoregulation between different domains of PLC ϵ . Clearly, further study is necessary to investigate how PLC ϵ second messengers could promote/inhibit endothelial barrier stability, as well as determine under what conditions (i.e. subcellular/microdomain localization of PLC ϵ) lipase activity positively or negatively affects endothelial barrier function.

Dusaban et al also observed that activation of PLC ϵ leads to sustained Rap1 activation[44], which would likely have a major effect on cell adhesion in endothelial cells. As Rap1 is a key regulator of adherens junction stability and integrin activation, cell-cell and cell-extracellular matrix adhesion would likely be increased. Similarly, in neonatal rat ventricular myocytes, PLC ϵ is vital for maintaining sustained Rap1 activation[4]. In myocytes, this leads to increased

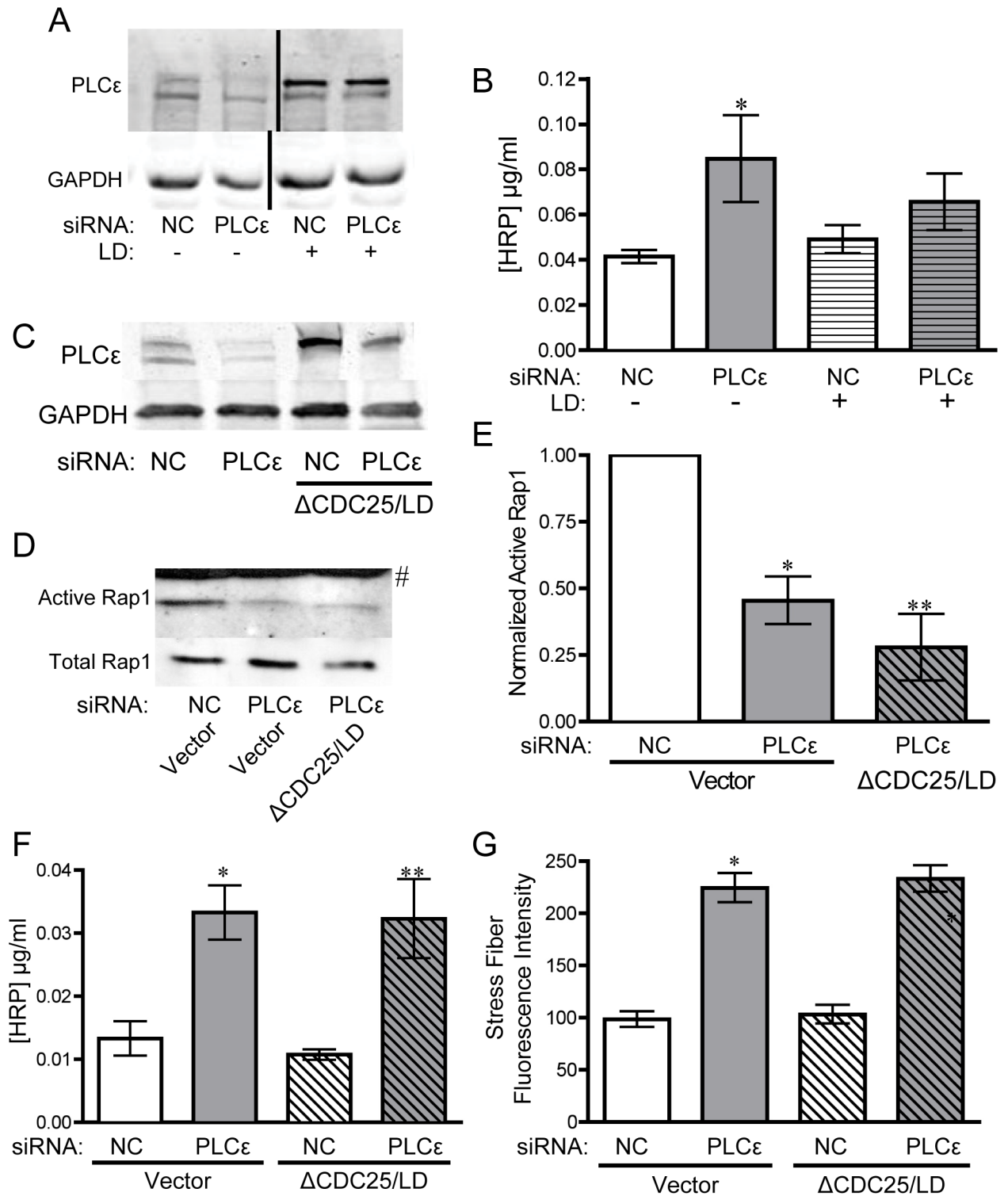


Fig 5. PLCε lacking the CDC25 domain and lipase activity cannot rescue monolayer integrity and decreased active Rap1 levels. **A)** PLCε expression in HPAEC infected with NC or PLCε siRNA ± PLCε lipase dead. Blots are representative. **B)** HRP leak through an HPAEC monolayer infected with negative control NC or PLCε siRNA ± PLCε lipase dead (LD). Data shown are the mean HRP concentration, ± SEM. n = 6, p = 0.002 by ANOVA, *p < 0.001 by post-hoc test vs. NC infected cells. **C)** PLCε expression in HPAEC infected with NC or PLCε siRNA ± ΔCDC25/LD. Blots are representative, n = 3. **D)** Active Rap1 pull-down assay from lysates infected with negative control or PLCε siRNA ± ΔCDC25/LD. Blots are representative, n = 3. **E)** Densitometric quantification of blots in (D). Data shown are active Rap1 normalized to total Rap1 ± SEM, n = 3, p = 0.0007 by ANOVA, *p < 0.01 vs. NC infected cells by post-hoc test, and

p<0.001 vs. NC siRNA infected cells. # indicates band from non-specific secondary antibody. All blots used for quantification can be found in [S8 Fig](#). **F) HRP leak through HPAEC monolayer infected with negative control (NC) or PLCε siRNA ± PLCε ΔCDC25/lipase dead (ΔCDC25/LD). Data shown are the mean HRP concentration, ± SEM. n = 9, p<0.0001 by ANOVA, *p<0.001 by post-hoc test vs. NC infected cells. **G**) Fluorescent intensity quantification of images of NC or PLCε siRNA infected cells ± ΔCDC25/LD. n≥40 cells from 10 fields of view, p<0.0001 by ANOVA, *p<0.001 by post-hoc test vs. NC infected cells.

doi:10.1371/journal.pone.0162338.g005

PKD activation, hypertrophic gene up-regulation[42], and in astrocytes and inflamed endothelial cells, to activation of pro-inflammatory NFκB signaling[43,45]. We can only speculate about the potential for PKD activation in our system, but as PKD is thought to exert primarily pro-inflammatory effects on the endothelium, we would expect PLCε activity in endothelial cells would promote, not protect against, loss of barrier function, as was seen under inflammatory conditions[43]. This suggests that the outcome of PLCε activity is likely highly dependent on cell type and the local signaling environment.

Lastly, our studies show that PLCε lies upstream of KRIT1 signaling. Previous studies have shown that the KRIT1-Rap1 interaction and subsequent increase in membrane associated KRIT1 is important for the ability of Rap1 to limit monolayer leak[14,15]. Our study provides further evidence that KRIT1 is a key Rap1 effector for maintaining endothelial barrier function,. However, other Rap1 effectors, Rasip and Radil, have been implicated in the stabilization of the endothelial barrier by Rap1 [46,47], where they appear to have a similar function in blocking Rho activity as does KRIT1[17]. It is unknown whether Rasip/Radil are important Rap1 effectors downstream of PLCε activity, nor whether they act in parallel to KRIT1, or

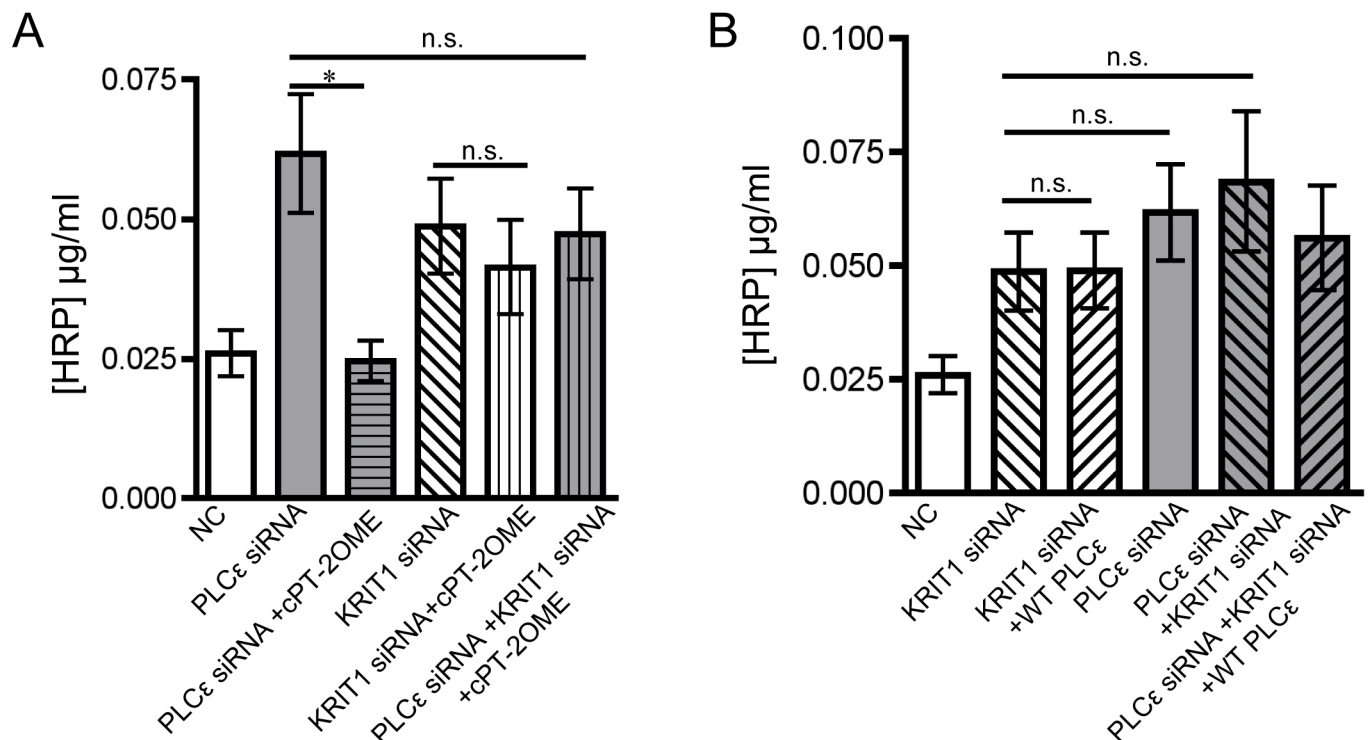


Fig 6. Loss of KRIT1 in PLCε depleted HPAEC prevents rescue by 8-pCPT-2'-O-Me-cAMP-AM and wild type PLCε. **A**) HRP leak through HPAEC monolayer infected with negative control (NC) or PLCε siRNA ± anti-KRIT1 siRNA or 1 μM 8-pCPT-2'-O-Me-cAMP-AM (cPT-2OME). Data shown are the mean HRP concentration, ± SEM. n = 9, p<0.0001 by ANOVA, *p<0.001 by post-hoc test vs. PLCε siRNA infected cells. n.s., non-significant. **B**) HRP leak through HPAEC monolayer infected with negative control (NC) or PLCε siRNA ± anti-KRIT1 siRNA or siRNA resistant PLCε (WT PLCε). Data shown are the mean HRP concentration, ± SEM. n = 9, p<0.0001 by ANOVA, n.s., non-significant.

doi:10.1371/journal.pone.0162338.g006

work synergistically. While our data clearly suggests that activation of the Rap1-KRIT1 signaling axis may be a widespread mechanism for regulating cell-cell contact, additional studies will be needed to assess a putative role for Rasip and Radil downstream of PLC ϵ .

Lastly, we do note that PLC ϵ knockout mice are viable and fertile[25], and exhibit none of the pathologies seen in KRIT1 or Rap1 loss-of-function mutants in mice and humans[48–53]. Thus PLC ϵ -dependent activation of the Rap1-KRIT1 signaling axis is dispensable during development and in adulthood, suggesting that redundant mechanisms are in place to activate Rap1. However, conditional PLC ϵ knockout models have shown significant differences with global knockout models. For example, global loss of PLC ϵ potentiates cardiac hypertrophy[25] while deletion of PLC ϵ in the heart limits it[42]. These divergent findings suggest that an endothelial specific PLC ϵ knockout may be required to fully explore the endothelial role of PLC ϵ .

In conclusion, our results have shown a novel role of PLC ϵ in the maintenance of endothelial barrier function, via its CDC25 GEF domain and lipase activity, and subsequent up-regulation of Rap1 activity. Although the involvement of the lipase domain is surprising, these data point to a potential ability of this enzyme to promote barrier integrity through calcium or DAG dependent mechanisms, and also support the idea that the function of PLC ϵ is cell type and context dependent. Given the thought-provoking role of PLC ϵ in basal and inflammatory endothelial barrier function, these findings may stimulate future research into the role of PLC ϵ in models of angiogenesis or vascular pathologies.

Supporting Information

S1 Fig. Knockdown of PLC ϵ does not increase 150kDa FITC-dextran flux. 150 kDa FITC-dextran leak through an HPAEC monolayer infected with negative control (NC) \pm 4U/ml thrombin or PLC ϵ siRNA. Data shown are RFU \pm SEM. n = 4.
(JPG)

S2 Fig. Knockdown of PLC ϵ reduces VE-cadherin junctional thickness. **A)** Western blot expression of VE-cadherin and GAPDH in HPAEC infected with infected with negative control (NC) or PLC ϵ siRNA \pm 1 μ M 8-pCPT-2'-O-Me-cAMP-AM (cPT-2OMe). Blots are representative, n = 3. **B)** Quantification of (A). Data shown are VE-cadherin normalized to GAPDH \pm SEM. n = 3. **C)** Fluorescent intensity quantification of images of NC or PLC ϵ siRNA infected cells \pm 1 μ M 8-pCPT-2'-O-Me-cAMP-AM (cPT-2OMe). n \geq 40 cells from 10 fields of view.
(JPG)

S3 Fig. The RA2 domain of PLC ϵ does not regulate monolayer integrity, basal Rap1 activity or stress fiber formation. **A)** HRP leak through HPAEC monolayer infected with negative control (NC) or PLC ϵ siRNA \pm PLC ϵ K2150E. Data shown are the mean HRP concentration, \pm SEM. n = 4. **B)** PLC ϵ expression in HPAEC infected with NC or PLC ϵ siRNA \pm PLC ϵ K2150E (RA2 binding-deficient). Blots are representative, n = 4. **C)** Densitometric quantification of active Rap1 pull-down assay from lysates infected with negative control or PLC ϵ siRNA \pm PLC ϵ K2150E. Data shown are active Rap1 normalized to total Rap1 \pm SEM, n = 4. **D)** Fluorescent intensity quantification of images of NC or PLC ϵ siRNA infected cells \pm PLC ϵ K2150E. n \geq 40 cells from 10 fields of view.
(JPG)

S4 Fig. Representative blot of KRIT1-depletion in Fig 6. Immunoprecipitation of KRIT1 from NC or PLC ϵ siRNA infected lysates \pm anti-KRIT1 siRNA, 1 μ M 8-pCPT-2'-O-Me-cAMP-AM, or siRNA resistant PLC ϵ (WT PLC ϵ). Blots are representative, n = 3.
(JPG)

S5 Fig. Western blots used for quantification in Fig 2A/2B.
(JPG)

S6 Fig. Western blots used for quantification in Fig 3A/3B.
(JPG)

S7 Fig. Western blots used for quantification in Fig 4B/4C.
(JPG)

S8 Fig. Western blots used for quantification in Fig 5D/5E.
(JPG)

Acknowledgments

We would like to thank Dr. Sundeep Malik for making the PLC ϵ Δ CDC25/lipase dead adenovirus and providing the NRVF lysate, and Dr. Craig Nash for providing the PLC $\epsilon^{-/-}$ heart lysate.

Author Contributions

Conceptualization: AS AJG.

Formal analysis: PD AJG.

Funding acquisition: AJG.

Investigation: PD.

Methodology: PD AJG.

Project administration: AJG.

Resources: AS AJG.

Supervision: AJG.

Validation: PD AJG.

Visualization: PD AJG.

Writing – original draft: PD AJG.

Writing – review & editing: AS PD AJG.

References

1. Smrcka AV, Brown JH, Holz GG. Role of phospholipase C ϵ in physiological phosphoinositide signaling networks. *Cellular Signalling*. 2012 Jun; 24(6):1333–43. doi: [10.1016/j.cellsig.2012.01.009](https://doi.org/10.1016/j.cellsig.2012.01.009) PMID: [22286105](https://pubmed.ncbi.nlm.nih.gov/22286105/)
2. Park JB, Lee CS, Jang J-H, Ghim J, Kim Y-J, You S, et al. Phospholipase signalling networks in cancer. *Nat Rev Cancer*. 2012 Nov; 12(11):782–92. doi: [10.1038/nrc3379](https://doi.org/10.1038/nrc3379) PMID: [23076158](https://pubmed.ncbi.nlm.nih.gov/23076158/)
3. Jin T-G, Satoh T, Liao Y, Song C, Gao X, Kariya K-I, et al. Role of the CDC25 homology domain of phospholipase Cepsilon in amplification of Rap1-dependent signaling. *J Biol Chem*. 2001 Aug 10; 276(32):30301–7. PMID: [11395506](https://pubmed.ncbi.nlm.nih.gov/11395506/)
4. Oestreich EA, Malik S, Goonasekera SA, Blaxall BC, Kelley GG, Dirksen RT, et al. Epac and Phospholipase C Regulate Ca²⁺ Release in the Heart by Activation of Protein Kinase C and Calcium-Calmodulin Kinase II. *Journal of Biological Chemistry*. 2008 Nov 20; 284(3):1514–22. doi: [10.1074/jbc.M806994200](https://doi.org/10.1074/jbc.M806994200) PMID: [18957419](https://pubmed.ncbi.nlm.nih.gov/18957419/)
5. Kelley GG, Reks SE, Ondrako JM, Smrcka AV. Phospholipase C(epsilon): a novel Ras effector. *EMBO J*. 2001 Feb 15; 20(4):743–54. PMID: [11179219](https://pubmed.ncbi.nlm.nih.gov/11179219/)

6. Seifert JP, Zhou Y, Hicks SN, Sondek J, Harden TK. Dual activation of phospholipase C-epsilon by Rho and Ras GTPases. *J Biol Chem*. 2008 Oct 31; 283(44):29690–8. doi: [10.1074/jbc.M805038200](https://doi.org/10.1074/jbc.M805038200) PMID: [18765661](https://pubmed.ncbi.nlm.nih.gov/18765661/)
7. Song C, Satoh T, Edamatsu H, Wu D, Tadano M, Gao X, et al. Differential roles of Ras and Rap1 in growth factor-dependent activation of phospholipase Cε. *Oncogene*. Nature Publishing Group; 2002 Nov 21; 21(53):8105–13.
8. Kelley GG, REKS SE, Smrcka AV. Hormonal regulation of phospholipase Cepsilon through distinct and overlapping pathways involving G12 and Ras family G-proteins. *Biochem J*. 2004 Feb 15; 378(Pt 1):129–39. PMID: [14567755](https://pubmed.ncbi.nlm.nih.gov/14567755/)
9. Bunney TD, Harris R, Gandarillas NL, Josephs MB, Roe SM, Sorli SC, et al. Structural and mechanistic insights into ras association domains of phospholipase C epsilon. *Molecular Cell*. 2006 Feb 17; 21(4):495–507. PMID: [16483931](https://pubmed.ncbi.nlm.nih.gov/16483931/)
10. Cullere X, Shaw SK, Andersson L, Hirahashi J, Lusinskas FW, Mayadas TN. Regulation of vascular endothelial barrier function by Epac, a cAMP-activated exchange factor for Rap GTPase. *Blood*. 2005 Mar 1; 105(5):1950–5. PMID: [15374886](https://pubmed.ncbi.nlm.nih.gov/15374886/)
11. Pannekoek W-J, van Dijk JGG, Chan OYA, Huvneers S, Linnemann JR, Spanjaard E, et al. Epac1 and PDZ-GEF cooperate in Rap1 mediated endothelial junction control. *Cellular Signalling*. 2011 Dec; 23(12):2056–64. doi: [10.1016/j.cellsig.2011.07.022](https://doi.org/10.1016/j.cellsig.2011.07.022) PMID: [21840392](https://pubmed.ncbi.nlm.nih.gov/21840392/)
12. Glading A, Han J, Stockton RA, Ginsberg MH. KRIT-1/CCM1 is a Rap1 effector that regulates endothelial cell cell junctions. *The Journal of Cell Biology*. 2007 Oct 22; 179(2):247–54. PMID: [17954608](https://pubmed.ncbi.nlm.nih.gov/17954608/)
13. Chrzanowska-Wodnicka M, White GC, Quilliam LA, Whitehead KJ. Small GTPase Rap1 Is Essential for Mouse Development and Formation of Functional Vasculature. *PLoS ONE*. 2015; 10(12): e0145689. doi: [10.1371/journal.pone.0145689](https://doi.org/10.1371/journal.pone.0145689) PMID: [26714318](https://pubmed.ncbi.nlm.nih.gov/26714318/)
14. Liu JJ, Stockton RA, Gingras AR, Ablooglu AJ, Han J, Bobkov AA, et al. A mechanism of Rap1-induced stabilization of endothelial cell-cell junctions. *Molecular Biology of the Cell*. 2011 Jul 13; 22(14):2509–19. doi: [10.1091/mbc.E11-02-0157](https://doi.org/10.1091/mbc.E11-02-0157) PMID: [21633110](https://pubmed.ncbi.nlm.nih.gov/21633110/)
15. Meliton A, Meng F, Tian Y, Shah AA, Birukova AA, Birukov KG. Role of Krev Interaction Trapped-1 in Prostacyclin-Induced Protection against Lung Vascular Permeability Induced by Excessive Mechanical Forces and Thrombin Receptor Activating Peptide 6. *Am J Respir Cell Mol Biol*. 2015 Dec; 53(6):834–43. doi: [10.1165/rcmb.2014-0376OC](https://doi.org/10.1165/rcmb.2014-0376OC) PMID: [25923142](https://pubmed.ncbi.nlm.nih.gov/25923142/)
16. DiStefano PV, Kuebel JM, Sarelius IH, Glading AJ. KRIT1 Protein Depletion Modifies Endothelial Cell Behavior via Increased Vascular Endothelial Growth Factor (VEGF) Signaling. *Journal of Biological Chemistry*. 2014 Nov 21; 289(47):33054–65. doi: [10.1074/jbc.M114.582304](https://doi.org/10.1074/jbc.M114.582304) PMID: [25320085](https://pubmed.ncbi.nlm.nih.gov/25320085/)
17. Stockton RA, Shenkar R, Awad IA, Ginsberg MH. Cerebral cavernous malformations proteins inhibit Rho kinase to stabilize vascular integrity. *Journal of Experimental Medicine*. 2010 Apr 12; 207(4):881–96. doi: [10.1084/jem.20091258](https://doi.org/10.1084/jem.20091258) PMID: [20308363](https://pubmed.ncbi.nlm.nih.gov/20308363/)
18. Corr M, Lerman I, Keubel JM, Ronacher L, Misra R, Lund F, et al. Decreased krev interaction-trapped 1 expression leads to increased vascular permeability and modifies inflammatory responses in vivo. *Arterioscler Thromb Vasc Biol*. 2012 Nov; 32(11):2702–10. doi: [10.1161/ATVBAHA.112.300115](https://doi.org/10.1161/ATVBAHA.112.300115) PMID: [22922958](https://pubmed.ncbi.nlm.nih.gov/22922958/)
19. Glading AJ, Ginsberg MH. Rap1 and its effector KRIT1/CCM1 regulate β-catenin signaling. *Dis Model Mech*. The Company of Biologists Limited; 2010; 3(1–2):73–83.
20. Lopez I, Mak EC, Ding J, Hamm HE, Lomasney JW. A novel bifunctional phospholipase c that is regulated by Galpha 12 and stimulates the Ras/mitogen-activated protein kinase pathway. *Journal of Biological Chemistry*. 2001 Jan 26; 276(4):2758–65. PMID: [11022047](https://pubmed.ncbi.nlm.nih.gov/11022047/)
21. Kelley GG, Kaproth-Joslin KA, REKS SE, Smrcka AV, Wojcikiewicz RJH. G-protein-coupled receptor agonists activate endogenous phospholipase Cepsilon and phospholipase Cbeta3 in a temporally distinct manner. *Journal of Biological Chemistry*. 2006 Feb 3; 281(5):2639–48. PMID: [16314422](https://pubmed.ncbi.nlm.nih.gov/16314422/)
22. Citro S, Malik S, Oestreich EA, Radeff-Huang J, Kelley GG, Smrcka AV, et al. Phospholipase Cepsilon is a nexus for Rho and Rap-mediated G protein-coupled receptor-induced astrocyte proliferation. *Proc Natl Acad Sci USA*. 2007 Sep 25; 104(39):15543–8. PMID: [17878312](https://pubmed.ncbi.nlm.nih.gov/17878312/)
23. Dzhura I, Chepurny OG, Kelley GG, Leech CA, Roe MW, Dzhura E, et al. Epac2-dependent mobilization of intracellular Ca²⁺ by glucagon-like peptide-1 receptor agonist exendin-4 is disrupted in β-cells of phospholipase C-ε knockout mice. *J Physiol (Lond)*. 2010 Dec 15; 588(Pt 24):4871–89.
24. Zhang L, Malik S, Kelley GG, Kapiloff MS, Smrcka AV. Phospholipase C epsilon scaffolds to muscle-specific A kinase anchoring protein (mAkapbeta) and integrates multiple hypertrophic stimuli in cardiac myocytes. *Journal of Biological Chemistry*. 2011 Jul 1; 286(26):23012–21. doi: [10.1074/jbc.M111.231993](https://doi.org/10.1074/jbc.M111.231993) PMID: [21550986](https://pubmed.ncbi.nlm.nih.gov/21550986/)

25. Wang H, Oestreich EA, Maekawa N, Bullard TA, Vikstrom KL, Dirksen RT, et al. Phospholipase C epsilon modulates beta-adrenergic receptor-dependent cardiac contraction and inhibits cardiac hypertrophy. *Circulation Research*. 2005 Dec 9; 97(12):1305–13. PMID: [16293787](#)
26. Béziau DM, Toussaint F, Blanchette A, Dayeh NR, Charbel C, Tardif J-C, et al. Expression of phosphoinositide-specific phospholipase C isoforms in native endothelial cells. *PLoS ONE*. 2015; 10(4): e0123769. doi: [10.1371/journal.pone.0123769](#) PMID: [25875657](#)
27. Lo Vasco VR, Pacini L, Di Raimo T, D'arcangelo D, Businaro R. Expression of phosphoinositide-specific phospholipase C isoforms in human umbilical vein endothelial cells. *J Clin Pathol*. 2011 Oct; 64(10):911–5. doi: [10.1136/jclinpath-2011-200096](#) PMID: [21742750](#)
28. Sorli SC, Bunnay TD, Sugden PH, Paterson HF, Katan M. Signaling properties and expression in normal and tumor tissues of two phospholipase C epsilon splice variants. *Oncogene*. 2005 Jan 6; 24(1):90–100. PMID: [15558028](#)
29. Chrzanowska-Wodnicka M, Burrige K. Rho-stimulated contractility drives the formation of stress fibers and focal adhesions. *The Journal of Cell Biology*. 1996 Jun; 133(6):1403–15. PMID: [8682874](#)
30. Ridley AJ, Hall A. The small GTP-binding protein rho regulates the assembly of focal adhesions and actin stress fibers in response to growth factors. *Cell*. 1992 Aug 7; 70(3):389–99. PMID: [1643657](#)
31. Vliem MJ, Ponsioen B, Schwede F, Pannekoek W-J, Riedl J, Kooistra MRH, et al. 8-pCPT-2'-O-Me-cAMP-AM: an improved Epac-selective cAMP analogue. *Chembiochem*. 2008 Sep 1; 9(13):2052–4. doi: [10.1002/cbic.200800216](#) PMID: [18633951](#)
32. Borikova AL, Dibble CF, Sciaky N, Welch CM, Abell AN, Bencharit S, et al. Rho kinase inhibition rescues the endothelial cell cerebral cavernous malformation phenotype. *J Biol Chem*. 2010 Apr 16; 285(16):11760–4. doi: [10.1074/jbc.C109.097220](#) PMID: [20181950](#)
33. Hoepfner LH, Phoenix KN, Clark KJ, Bhattacharya R, Gong X, Sciuto TE, et al. Revealing the role of phospholipase Cβ3 in the regulation of VEGF-induced vascular permeability. *Blood*. 2012 Sep 13; 120(11):2167–73. doi: [10.1182/blood-2012-03-417824](#) PMID: [22674805](#)
34. Usatyuk PV, Kotha SR, Parinandi NL, Natarajan V. Phospholipase D signaling mediates reactive oxygen species-induced lung endothelial barrier dysfunction. *Pulm Circ*. 2013 Jan; 3(1):108–15. doi: [10.4103/2045-8932.109925](#) PMID: [23662182](#)
35. Zeiller C, Mebarek S, Jaafar R, Pirola L, Lagarde M, Prigent A-F, et al. Phospholipase D2 regulates endothelial permeability through cytoskeleton reorganization and occludin downregulation. *Biochim Biophys Acta*. 2009 Jul; 1793(7):1236–49. doi: [10.1016/j.bbamer.2009.04.001](#) PMID: [19371764](#)
36. Pappa V, Seydel K, Gupta S, Feintuch CM, Potchen MJ, Kampondeni S, et al. Lipid metabolites of the phospholipase A2 pathway and inflammatory cytokines are associated with brain volume in paediatric cerebral malaria. *Malar J*. 2015; 14:513. doi: [10.1186/s12936-015-1036-1](#) PMID: [26691993](#)
37. Tirupathi C, Minshall RD, Paria BC, Vogel SM, Malik AB. Role of Ca²⁺ signaling in the regulation of endothelial permeability. *Vascul Pharmacol*. 2002 Nov; 39(4–5):173–85. PMID: [12747958](#)
38. Sumagin R, Lomakina E, Sarelis IH. Leukocyte-endothelial cell interactions are linked to vascular permeability via ICAM-1-mediated signaling. *Am J Physiol Heart Circ Physiol*. 2008 Sep; 295(3):H969–77. doi: [10.1152/ajpheart.00400.2008](#) PMID: [18641276](#)
39. Bogatcheva NV, Verin AD, Wang P, Birukova AA, Birukov KG, Mirzopoyazova T, et al. Phorbol esters increase MLC phosphorylation and actin remodeling in bovine lung endothelium without increased contraction. *Am J Physiol Lung Cell Mol Physiol*. 2003 Aug; 285(2):L415–26. PMID: [12740219](#)
40. Bokhari SM, Zhou L, Karasek MA, Paturi SG, Chaudhuri V. Regulation of skin microvasculature angiogenesis, cell migration, and permeability by a specific inhibitor of PKCα. *J Invest Dermatol*. 2006 Feb; 126(2):460–7. PMID: [16374459](#)
41. Tinsley JH, Teasdale NR, Yuan SY. Involvement of PKCδ and PKD in pulmonary microvascular endothelial cell hyperpermeability. *Am J Physiol Cell Physiol*. 2004 Jan; 286(1):C105–11. PMID: [13679307](#)
42. Zhang L, Malik S, Pang J, Wang H, Park KM, Yule DI, et al. Phospholipase Cε hydrolyzes perinuclear phosphatidylinositol 4-phosphate to regulate cardiac hypertrophy. *Cell*. 2013 Mar 28; 153(1):216–27. doi: [10.1016/j.cell.2013.02.047](#) PMID: [23540699](#)
43. Bijli KM, Fazal F, Slavin SA, Leonard A, Grose V, Alexander WB, et al. Phospholipase C-ε signaling mediates endothelial cell inflammation and barrier disruption in acute lung injury. *Am J Physiol Lung Cell Mol Physiol*. 2016 Aug 1; 311(2):L517–24. doi: [10.1152/ajplung.00069.2016](#) PMID: [27371732](#)
44. Dusaban SS, Kunkel MT, Smrcka AV, Brown JH. Thrombin promotes sustained signaling and inflammatory gene expression through the CDC25 and Ras-associating domains of phospholipase Cε. *J Biol Chem*. 2015 Oct 30; 290(44):26776–83. doi: [10.1074/jbc.M115.676098](#) PMID: [26350460](#)

45. Dusaban SS, Purcell NH, Rockenstein E, Masliah E, Cho MK, Smrcka AV, et al. Phospholipase C epsilon links G protein-coupled receptor activation to inflammatory astrocytic responses. *Proc Natl Acad Sci USA*. 2013 Feb 26; 110(9):3609–14. doi: [10.1073/pnas.1217355110](https://doi.org/10.1073/pnas.1217355110) PMID: [23401561](https://pubmed.ncbi.nlm.nih.gov/23401561/)
46. Post A, Pannekoek W-J, Ross SH, Verlaan I, Brouwer PM, Bos JL. Rasip1 mediates Rap1 regulation of Rho in endothelial barrier function through ArhGAP29. *Proc Natl Acad Sci USA*. 2013 Jul 9; 110(28):11427–32. doi: [10.1073/pnas.1306595110](https://doi.org/10.1073/pnas.1306595110) PMID: [23798437](https://pubmed.ncbi.nlm.nih.gov/23798437/)
47. Post A, Pannekoek WJ, Ponsioen B, Vliem MJ, Bos JL. Rap1 Spatially Controls ArhGAP29 To Inhibit Rho Signaling during Endothelial Barrier Regulation. *Molecular and Cellular Biology*. 2015 Jul; 35(14):2495–502. doi: [10.1128/MCB.01453-14](https://doi.org/10.1128/MCB.01453-14) PMID: [25963656](https://pubmed.ncbi.nlm.nih.gov/25963656/)
48. Clatterbuck RE, Eberhart CG, Crain BJ, Rigamonti D. Ultrastructural and immunocytochemical evidence that an incompetent blood-brain barrier is related to the pathophysiology of cavernous malformations. *J Neurol Neurosurg Psychiatr*. 2001 Aug; 71(2):188–92. PMID: [11459890](https://pubmed.ncbi.nlm.nih.gov/11459890/)
49. Sahoo T, Goenaga-Diaz E, Serebriiskii IG, Thomas JW, Kotova E, Cuellar JG, et al. Computational and experimental analyses reveal previously undetected coding exons of the KRIT1 (CCM1) gene. *Genomics*. 2001 Jan 1; 71(1):123–6. PMID: [11161805](https://pubmed.ncbi.nlm.nih.gov/11161805/)
50. Mleynek TM, Chan AC, Redd M, Gibson CC, Davis CT, Shi DS, et al. Lack of CCM1 induces hyper-sprouting and impairs response to flow. *Hum Mol Genet*. 2014 Dec 1; 23(23):6223–34. doi: [10.1093/hmg/ddu342](https://doi.org/10.1093/hmg/ddu342) PMID: [24990152](https://pubmed.ncbi.nlm.nih.gov/24990152/)
51. Maddaluno L, Rudini N, Cuttano R, Bravi L, Giampietro C, Corada M, et al. EndMT contributes to the onset and progression of cerebral cavernous malformations. *Nature*. 2013 Jun 27; 498(7455):492–6. doi: [10.1038/nature12207](https://doi.org/10.1038/nature12207) PMID: [23748444](https://pubmed.ncbi.nlm.nih.gov/23748444/)
52. Whitehead KJ, Plummer NW, Adams JA, Marchuk DA, Li DY. Ccm1 is required for arterial morphogenesis: implications for the etiology of human cavernous malformations. *Development*. 2004 Mar; 131(6):1437–48. PMID: [14993192](https://pubmed.ncbi.nlm.nih.gov/14993192/)
53. Chrzanowska-Wodnicka M, Kraus AE, Gale D, White GC, VanSluys J. Defective angiogenesis, endothelial migration, proliferation, and MAPK signaling in Rap1b-deficient mice. *Blood*. 2008 Mar 1; 111(5):2647–56. PMID: [17993608](https://pubmed.ncbi.nlm.nih.gov/17993608/)